J Therm Anal Calorim (2012) 110:611–617
DOI 10.1007/s10973-011-2018-3

Thermogravimetry study of pyrolytic characteristics and kinetics of the giant wetland plant *Phragmites australis*

Hui Zhao · Huaxiao Yan · Congwang Zhang · Binbin Sun · Yan Zhang · Shuangshuang Dong · Yanhui Xue · Song Qin

Received: 21 August 2011 / Accepted: 19 October 2011 / Published online: 12 November 2011

Abstract The pyrolytic characteristics and kinetics of wetland plant *Phragmites australis* was investigated using thermogravimetric method from 50 to 800 °C in an inert argon atmosphere at different heating rates of 5, 10, 25, 30, and 50 °C min^{-1}. The kinetic parameters of activation energy and frequency factor were deduced by appropriate methods. The results showed that three stages appeared in the thermal degradation process. The most probable mechanism functions were described, and the average apparent activation energy was deduced as 291.8 kJ mol^{-1}, and corresponding pre-exponential factors were determined as well. The results suggested that the most probable reaction mechanisms could be described by different models within different temperature ranges. It showed that the apparent activation energies and the corresponding pre-exponential factors could be obtained at different conversion rates. The results suggested that the experimental results and kinetic parameters provided useful information for the design of pyrolytic processing system using *P. australis* as feedstock.

Keywords Biomass · *Phragmites australis* · Pyrolysis · Kinetics · TG

Introduction

In recent years, biomass as a promising renewable energy source has received considerable attention because supplies of fossil fuels are dwindling and price just as energy demand continues to soar. Biomass is utterly unparalleled in many respects compared with fossil fuels [1]. Not only it can be used and regenerated continuously as a renewable resource, but also it is important for CO_2 mitigation from the atmosphere. Meanwhile, contradictions between biomass supplying for bio-fuel production and food production have been intensified over the last few years, and it highlighted a huge potential and necessity of inedible biomass resources to produce bioenergy, such as *Miscanthus*, switchgrass (*Panicum virgatum*) [2–4].

Phragmites australis, a kind of non-edible biomass resource, is a cosmopolitan species of giant wetland plant native to every continent but Antarctica. Furthermore, *P. australis* has ever multiplied wildly as an invasive species with rapid growth, causing a serious environmental issue throughout the world [5]. More to the point, throughout the late autumn and winter, *P. australis* is losing green and becomes drying under natural conditions, which makes *P. australis* one of the best natural feedstock for pyrolysis without special technical process about energy-wasting dewatering. *P. australis* seems to be especially a promising energy plant and chemical feedstock due to its high production potential. Various processes have been proposed

H. Yan and C. Zhang contributed equally as first authors.

H. Zhao (✉) · H. Yan · C. Zhang · B. Sun · Y. Zhang · S. Dong · Y. Xue
College of Chemical and Environmental Engineering, Shandong University of Science and Technology, Qingdao 266590, People's Republic of China
e-mail: zhsdust@126.com

H. Zhao · H. Yan · C. Zhang · B. Sun · Y. Zhang · S. Dong · Y. Xue
Shandong Provincial Key Laboratory of Low-carbon Energy Chemical Engineering, Qingdao 266590, People's Republic of China

S. Qin
Bioresources Lab, Yantai Institute of Coastal Zone Research, Chinese Academy of Sciences, Yantai 264003, Shandong, People's Republic of China

for the integrated utilization of these powerful plants. It is reported that *P. australis* (common reed) can provide up to 18−28 tons of dry mass per acre per year as an invasive perennial weed [35]. *P. australis* is becoming very important as a stable biomass source for China with its natural huge reserves and increasing artificial cultivation.

Recently, various processes have been proposed for the comprehensive utilization of biomass [6, 7]. Biomass pyrolysis has demonstrated itself to be a kind of biomass-energy utilization technology which transforms low-energy density biomass materials into high-energy density liquid products which can be utilized more efficiently in an environment-friendly manner.

A thorough knowledge of the thermal behavior and pyrolysis kinetics of biomass are required for the proper design and operation of the pyrolysis conversion systems. Thermogravimetry (TG) was selected for the thermal decomposition process. The kinetic data from TG are not only very useful for understanding the thermal degradation processes and mechanisms, but also can be used as input parameters for a thermal degradation reaction system. Extensive literature has been published on the experiments and mechanism aspects of a great range of biomass, such as waste woods, agricultural residues, and municipal solid wastes [8–13]. However, although Sutcu (2008) has investigated the pyrolysis of *P. australis* and characterization of liquid and solid products [14], there is currently no information available on the pyrolysis kinetics of *P. australis* until now.

In this study, pyrolytic kinetics of *P. australis* was investigated using non-isothermal TG method. The characteristics of the thermal degradation at different heating rates under an inert atmosphere were studied. The objective of this study was to obtain the kinetic parameters of the decomposition and then to determine the thermal degradation mechanism.

Materials and methods

Material

Phragmites australis samples were collected from a wetland near the campus of Shandong University of Science and Technology, Qingdao, China, September 2010. The samples were sun dried for 10 days, after which the samples were pulverized in a plant disintegrator to all passing a 120 mesh sieve. All samples were stored in a desiccator.

The samples were analyzed to determine the main properties that affect thermal conversion. Proximate analysis was carried out according to national standard GB212-91 (China). Ultimate analysis was measured by Element Analysensysteme GmbH vario EL cube. Cellulose, hemicellulose, and lignin contents were analyzed according to the method described in literature [15]. The results are summarized in Table 1. All measurements were replicated three times.

Pyrolysis of the samples

TG analyses were carried out using a thermal analyzer (TGA/DSC1/1600LF, METTLER TOLEDO Co., Switzerland). Initial sample masses of 10 mg were pyrolyzed under an argon flow rate of 50 cm^3 min^{-1} with a heating rate of 5, 10, 25, 30, and 50 °C min^{-1}. The mass loss and calorific changes in response to temperatures were then recorded and used to plot the TG, derivative thermogravimetric (DTG) and differential scanning calorimetric (DSC) curves. All experiments were replicated three times. All profiles were not presented here for concision, because the profile of 25 °C min^{-1} can be one perfect representative.

Kinetic parameters of the pyrolysis

Calculation of activation energy

The rate constant is a non-linear function of α and T, which can be expressed as

$$\frac{d\alpha}{dt} = k(T)f(\alpha) \tag{1}$$

where α defined as

$$\alpha = \frac{m_0 - m}{m_0 - m_\infty}, \tag{2}$$

is the conversion rate. where m_0, m, and m_∞ refer to the initial, actual, and final residual mass of the sample, respectively.

If the heating rate β is a constant, $\beta = dT/dt$, then Eq. 1 can be reformulated as

$$\beta\frac{d\alpha}{dT} = k(T)f(\alpha) \tag{3}$$

Eq. 3 can be rewritten as follows:

$$\frac{d\alpha}{f(\alpha)} = \frac{1}{\beta}k(T)dT \tag{4}$$

The reaction rate $k(T)$ calculated by Arrhenius equation $\left(k(T) = Ae^{-\frac{E_a}{RT}}\right)$ and the mechanism function, $f(\alpha)$ is involved in Eq. 4.

The Arrhenius equation was substituted into Eq. 4, then we can get

Table 1 Main characteristics of *P. australis* biomass

Parameters	*P. australis*
Proximate analysis[a]/wt%, ad. basis	
Moisture	5.89 ± 0.03
Ash	12.32 ± 1.12
Volatile matter	70.01 ± 2.40
Fix carbon[c]	11.78
Ultimate analysis[b]/wt%, daf. Basis	
Carbon	42.78 ± 1.53
Hydrogen	5.17 ± 0.02
Oxygen[c]	50.511
Nitrogen	1.31 ± 0.02
Sulfur	0.229 ± 0.01
C/H	8.31 ± 0.31
C/N	32.57 ± 1.55
Component analysis/wt%, daf. basis	
Hemicellulose	30.68 ± 3.15
Lignin	20.34 ± 1.56
Cellulose	43.05 ± 3.98

[a] Dry free basis

[b] Dry ash free basis

[c] Calculated by difference

$$\frac{\mathrm{d}\alpha}{f(\alpha)} = \frac{1}{\beta} A e^{-\frac{E_a}{RT}} \mathrm{d}T. \tag{5}$$

The integral form of Eq. 5 can be described as

$$g(\alpha) = \int_0^{\alpha} \frac{\mathrm{d}\alpha}{f(\alpha)} = \frac{1}{\beta} \int_{T_0}^{T} A e^{-\frac{E_a}{RT}} \mathrm{d}T = \frac{AE_a}{\beta R} P(x) \tag{6}$$

In Eq. 6, T_0 and T are the initial and actual temperature, respectively, corresponding to the initial and actual conversion rate.

The function of $p(x)$ ($x = E_a/RT$) has the approximate equations, which can be expressed as follows:

$$p(x) = \frac{\exp(-x)}{x^2} \tag{7}$$

$$p(x) = 0.0048 \exp(-1.0516x) \tag{8}$$

The ratios of $P(x)$ and Eq. 7, $P(x)$ and Eq. 8 defined as $h(x)$, $H(x)$, respectively, can be described by the following expression:

$$h(x) = \frac{P(x)}{\frac{1}{x^2}\exp(-x)}, \tag{9}$$

$$H(x) = \frac{P(x)}{0.0048 \exp(-1.0516x)} \tag{10}$$

By undergoing simple transformations, we can get the following Eq. 11:

$$H(x) = \frac{P(x)}{0.0048 \exp(-1.0516x)} = \frac{\exp(-x)h(x)}{0.0048x^2 \exp(-1.0516x)} \tag{11}$$

$$h(x) = \frac{x^4 + 18x^3 + 86x^2 + 96x}{x^4 + 20x^3 + 120x^2 + 240x + 120} \tag{12}$$

Substitution of Eqs. 11 and 12 into Eq. 6 gives:

$$\ln \frac{\beta}{H(x)} = \ln \left[\frac{0.0048AE_a}{g(\alpha)R} \right] - 1.0516 \frac{E_a}{RT} \tag{13}$$

$$\ln \frac{\beta}{h(x)T^2} = \ln \left[\frac{AR}{E_a g(\alpha)} \right] - \frac{E_a}{RT} \tag{14}$$

A method derived from an iteration Eqs. 13 or 14 for calculation of the activation energy E_a is used. The iterative process could be divided into three steps: First, the initial activation energy E_{a1} was calculated by assuming $h(x) = 1$ or $H(x) = 1$ with regard to Eqs. 13 or 14. Second, substitution of E_{a1} and temperature gradients with a given value of conversion rate and the dissimilar β in $x = E_a/RT$ can give x, then the apparent activation energy E_{a2} could be obtained from the scope of curve ($\ln \frac{\beta}{h(x)T^2}$ against $\frac{1}{T}$ or $\ln \frac{\beta}{H(x)}$ against $\frac{1}{T}$). Third, E_{a1} was replaced by E_{a2} and the second step was repeated continually until $E_{ai} - E_{ai-1} < 0.01$ kJ mol^{-1} [16].

Determination of the most probable mechanism

The integrated form of Eq.4 is generally expressed as

$$\int_{\alpha_m}^{\alpha_n} \frac{\mathrm{d}\alpha}{f(\alpha)} = \frac{1}{\beta} \int_{T_m}^{T_n} k(T) dT \tag{15}$$

α_m, α_n correspond to T_m, T_n, respectively. The left of the Eq. 15 can be defined as

$$F(\alpha)_{mn} = \int_{\alpha_m}^{\alpha_n} \frac{d\alpha}{f(\alpha)} \tag{16}$$

and the right of that can be defined as

$$I(T)_{mn} = \int_{T_m}^{T_n} k(T) \mathrm{d}T. \tag{17}$$

Therefore, the Eq. 15 can be rewritten as

$$F(\alpha)_{mn} = \frac{1}{\beta} I(T)_{mn}. \tag{18}$$

The correlativity of $F(\alpha)_{mn}$ and $1/\beta$ was analyzed using the unitary linear regression equation in various ranges of temperature.

Calculation of the pre-exponential factor

The pre-exponential factor A_1 and A_2 can be obtained from the intercept of Eqs. 13 and 14, respectively. The

determination of most probable mechanism was based on the correlativity of $F(\alpha)_{mn}$ and $1/\beta$, in control of the same α and diverse β. However, on average, the value of A_1 and A_2 was widely apart from each other obtained from Eqs. 13 and 14 so that the following method was employed to choose the probable A between A_1 and A_2 based on the proximity of the values of I with I_1 and I_2. First, making Arrhenius equation substituted into Eq. 15 can generate Eq. 19 which can be utilized to compute I_1 and I_2 with the acquired A, E_a, and $P(x)$.

$$I(T)_{mn} = \int_{T_m}^{T_n} k(T)dT = \frac{AE_a}{R}P(x)|_{x_m}^{x_n} \quad (19)$$

Second, according to Eq. 18, a plot of $F(\alpha)_{mn}$ versus $1/\beta$ gives straight line with an intercept of zero and slope of I. Third, A can be obtained by means of comparing the values of I with I_1 and I_2. The final A was selected from A_1 and A_2 according to the values of I_1 and I_2, corresponding to A_1 and A_2, which were more closely related to that of I and the corresponding pre-exponential factor as the final A. All plots were generated and the lines were fitted using the Origin 8.0 software (Origin Lab Co.).

Results and discussion

Material characterization

The results of proximate, ultimate, and component analysis of *P. australis* samples were summarized in Table 1. It showed a higher amount of ash and cellulose contents compared with other terrestrial materials (Olive residues that study by A. Aboulkas, and pistachio shell that study by Korkut Açıkalın) that came from other literatures [36, 37]. The volatile matter and lignin contents of *P. australis* were lower, while the sulfur content of the samples was approximately equal [11–13].

Characteristics of the thermal degradation process

Figure 1 showed the mass loss (X%) and the rate of mass loss ($-dX/dt$) curves derived from the pyrolysis of *P. australis* under argon atmosphere at the heating rate of 25 °C min^{-1} (All profiles were not presented here for concision). According to the changing rules of the curvilinear, three regions appeared in the pyrolytic process.

The first (I) region went from 50 to 200 °C. During this region, a slow ramp showed in the mass loss curve and a slight inferior fovea was observed in the rate of mass loss curve corresponding to the loss of water and devolatilization of the light molecules holding raw material mass about 6% of the left and right sides.

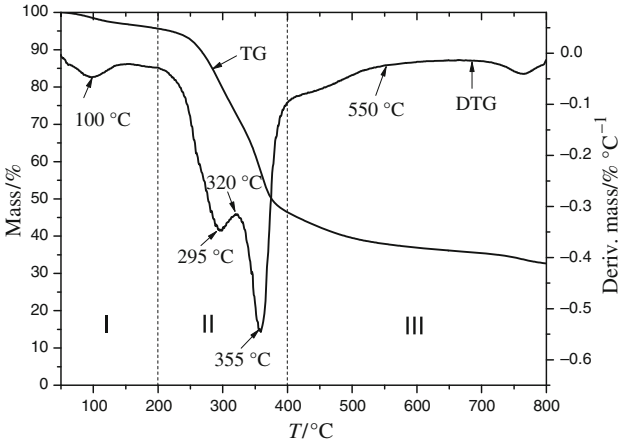

Fig. 1 TG/DTG curves of *P. australis* at heating rate of 25 °C min^{-1} (as an example for concision)

The second (II) region ranging from 200 to 400 °C was attributed to a sharp drop in mass loss curve and formation of the main thermal degradation product, corresponding to the degradation of hemicellulose and cellulose. Two different zones defined as first (I) zone occurred as the temperature increased from 200 to 320 °C with a maximum mass loss point at 295 °C and second (II) zone occurred as the temperature increased from 320 to 400 °C with a maximum mass loss point at 355 °C existing in region (II) in the rate of mass loss curve with quick velocity leading to the tremendous mass loss exceeding 50% of total volatiles. And in the third (III) region, the residuals were slowly decomposed from 400 °C to the final temperature 800 °C. The mass loss curve and the rate of mass loss curve tended to be flat, especially after 550 °C.

The region (II) corresponding to the main pyrolysis process was the major object of the study. The hemicellulose decomposed between 225 and 325 °C and the cellulose was found to decompose at around 325 to 375 °C. Lignin had a wide thermal degradation temperature ranges covering from 250 to 500 °C [17–19]. The maximum peak of the region (II) in the TG curve was related to the decomposition of cellulose and hemicellulose. Moreover, shouldering could be found before the major peak, nevertheless, pyrolysis processes of many kinds of biomass lack the side peak, as a result of discrepancy in the raw material compositions. The side peak in low temperatures zone corresponding to the decomposition of hemicelluloses, while the main peak in the high temperatures zone corresponding to the decomposition of cellulose. In addition, the peak of thermal degradation lignin could not be observed. The emergence of the side peak depended on the contents of hemicellulose and cellulose in the biomass components. The low content of hemicellulose components contributed to the merging of side peak into the main peak. Moreover, the relative height of the peak was proportional to the

reactive activities. For this reason, it indicated that a less volatile corresponding to the low reactive activities pulls the maximal pyrolytic velocity down. In other aspects, the temperature of initial decomposition and the maximal pyrolytic velocity had low relativity with the high amount of ashes which could strengthen the pyrogenation process as a catalyzer.

DTG curve (Fig. 2) had two extensive peaks between 200 and 400 °C, which were attributed to the decomposition of cellulose and hemicellulose. Obviously, the TG and DTG curves tended to shift to a greater range of temperature as the heating rate increased, which may be involved in a shorter retention time and greater thermal degradation temperature required for organic material, causing the maximum curve rate to spread to the right side. These tendencies were found analogous to those reported before [20–23] .

Kinetic analysis of the pyrolysis process

Different conversion rates at different heating rates and temperatures were obtained to determine kinetic parameters. The activation energy E_a could be obtained from the scope of the Eqs. 13 or 14 curve ($\ln\frac{\beta}{h(x)T^2}$ against $\frac{1}{T}$ or $\ln\frac{\beta}{H(x)}$ against $\frac{1}{T}$) using iterative method. Table 2 showed the activation energies obtained at different conversion rates.

The correlativity of $f(\alpha)_{mn}$ *and* $1/\beta$ was analyzed by the unitary linear regress equation in Eq. 18 at different temperature ranges in order to get the probable mechanism function. Moreover, the probable mechanism function corresponding to the correlation coefficient $R > 0.99$ chosen from the mechanism functions shown in references [21, 24–28, 38] at intervals of 5 K from 500 to 675 K. The results shown in Table 3 indicated that the probable mechanism function is distinct in different temperature ranges, reflecting the complexity of the reaction processes.

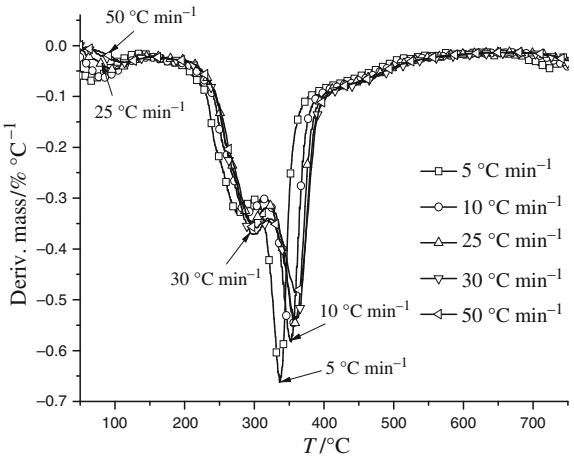

Fig. 2 DTG curves of *P. australis* at different heating rates

Table 2 The activation energy obtained at different conversion rates

Conversion rate/α	E_1/kJ mol^{-1}	R_1	E_2/kJ mol^{-1}	R_2
0.1	90.73	0.8133	90.73	0.7968
0.2	205.48	0.9732	205.51	0.9704
0.3	247.74	0.9829	247.76	0.9811
0.4	300.00	0.9795	300.04	0.9774
0.5	323.78	0.9607	323.84	0.9567
0.6	295.05	0.9614	295.09	0.9575
0.7	279.58	0.9813	279.62	0.9794
0.8	592.12	0.9492	592.22	0.9441
Average	291.81		291.85	

Table 3 The probable mechanism functions at different temperature ranges

T_m/K	T_n/K	R	Mechanism function
500	505	0.9909	Diffusion (Ginstling-Brounshtein equation): $G(\alpha) = (1-2\alpha/3)-(1-\alpha)^{2/3}$
515	520	0.9944	Limiting surface reaction between both phases (three dimensions): $G(\alpha) = 1-(1-\alpha)^{1/3}$
535	540	0.9975	Limiting surface reaction between both phases (One dimension): $G(\alpha) = \alpha$
575	580	0.9957	Diffusion (One-way transport): $G(\alpha) = \alpha^2$
580	585	0.9950	Order of reaction (Third-order): $G(\alpha) = [(1-\alpha)^{-2}-1]/2$
610	615	0.9948	Diffusion (Ginstling-Brounshtein equation): $G(\alpha) = (1-2\alpha/3)-(1-\alpha)^{2/3}$
615	620	0.9954	Order of reaction (Third-order): $G(\alpha) = [(1-\alpha)^{-2}-1]/2$

The reaction process is mainly elaborated by reaction orders, diffusion, and limiting surface reaction between both phases in different temperature ranges.

The pre-exponential factor A_1 and A_2 can be obtained from the intercept of Eqs. 13 and 14 with the acquired E_a and $f(\alpha)_{mn}$ if the same α and diverse β are controlled. The results on pre-exponential factor A_1 and A_2 were listed in Table 4.

According to Table 4, the values of pre-exponential factor A_1 and A_2 were widely apart from each other obtained from Eqs. 13 and 14. I_1, I_2 derived from solving Eq. 19 with the acquired pre-exponential factor A_1 and A_2. I can be obtained from solving the slope of Eq. 18. The specific methods had been concerned above.

The final A was selected from A_1 and A_2 according to I_1 and I_2 corresponding to A_1 and A_2. Concretely, the values of I_1 and I_2 which were more closely related to that of I were selected, and then the corresponding pre-exponential factor acted as the final A. The results were listed in Table 4.

Table 4 The pre-exponential factor A

Conversion rate/α	$\ln[\beta/H(x)] \sim 1/T$	$\ln[\beta/h(x)T^2] \sim 1/T$	
	$\ln A_1/\min^{-1}$	$\ln A_2/\min^{-1}$	$\ln A/\min^{-1}$
0.1	15.68885	−2.90772	15.68885
0.2	40.60023	20.37371	40.60023
0.3	47.20227	26.60380	47.20227
0.4	58.32543	37.46730	58.32543
0.5	61.98347	36.85131	61.98347
0.6	65.51026	37.51013	65.51026
0.7	71.33620	41.33606	71.33620
0.8	74.35784	44.35767	74.35784

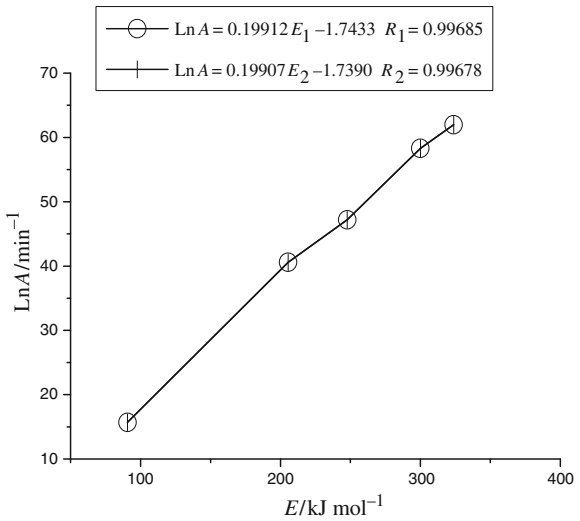

Fig. 3 The kinetic compensation effects

Figure 3 showed the kinetic compensation effects, $\ln A = 0.19912E_1 - 1.7433$, $\ln A = 0.19907E_2 - 1.739$, in response to pre-exponential factors and activation energy values. The related coefficient of pre-exponential factors and activation energy reaching 0.99 above indicate that the values of A and E are credible.

Comparison of various kinetic parameters including decomposition temperatures and activation energy of pyrolysis for different biomass [11, 22, 28–34]. The results indicated that the decomposition temperature of *P. australis* is higher than that of algae and lower than that of the higher plants. The activation energy of *P. australis* is higher than that of hemicellulose and lignin, but lower than that of cellulose. These findings also suggest that the thermal behavior is influenced greatly by the feedstock.

Conclusions

Phragmites australis was pyrolyzed in a TG analyzer from 50 to 800 °C at different heating rates of 5, 10, 25, 30, and 50 °C $\min^{-1}$. Three stages appeared in this thermal degradation process. TG and DTG curves tended to shift to a greater range of temperatures as the heating rates increased, causing the maximum curve rate to spread to the right. The most probable reaction mechanisms were described by different models between various temperature ranges. The apparent activation energies and the corresponding pre-exponential factors distributed in different alpha scopes were obtained.

Acknowledgements This study was financially supported by the National Natural Science Foundation of China (21076117), and CAS International Partnership Program "Typical environment processes and their effects on resources," and Outstanding young scholar fellowship of Shandong Province (JQ200914), and the Open Funding from the State Key Laboratory of Crop Biology in Shandong Agricultural University (2010KF06 and 2011KF14), and Projects of Shandong Province Higher Educational Science and Technology Program (J09LC22 and J10LC15), and the Open Funding from the Key Laboratory of Experimental Marine Biology, Institute of Oceanology (Kf201016), and Open Project Program of the Key Laboratory of Marine Bio-resources Sustainable Utilization (LMB101004), SCSIO, Chinese Academy of Sciences.

References

1. Demirbas A. Progress and recent trends in biofuels. Prog Energy Combust Sci. 2007;33:1–18.
2. Lewandowski I, Scurlock JMO, Lindvall E, Christou M. The development and current status of perennial rhizomatous grasses as energy crops in the US and Europe. Biom Bioen. 2003;25:335–61.
3. Basso MC, Cerrella EG, Buonomo EL, Bonelli PR, Cukierman AL. Thermochemical conversion of *Arundo donax* into useful solid products. Ener Sour. 2005;27:1429–38.
4. Sujjakulnukit B, Yingyuad R, Maneekhao V, Pongnarintasut V, Bhattacharya SC, Abdul Salam P. Assessment of sustainable energy potential of non-plantation biomass resources in Thailand. Biom Bioen. 2005;29:214–24.
5. Artigas F, Pechmann IC. Balloon imagery verification of remotely sensed *Phragmites australis* expansion in an urban estuary of New Jersey. Landsc Urban Plan. 2010;95:105–12.
6. Bridgwater T. Biomass for energy. J Sci Food Agr. 2006;86:1755–68.
7. Pevida C, Plaza MG, Arias B, Fermoso J, Rubiera F, Pis JJ. Surface modification of activated carbons for CO_2 capture. Appl Surf Sci. 2008;254:7165–72.
8. Erlich C, Björnbom E, Bolado D, Giner M, Fransson TH. Pyrolysis and gasification of pellets from sugarcane bagasse and wood. Fuel. 2006;85:1535–40.
9. Isci A, Demirer GN. Biogas production potential from cotton wastes. Renew Energy. 2007;32:750–7.
10. Lapuerta M, Hernández JJ, Rodríguez J. Comparison between the kinetics of devolatilization of forestry and agricultural wastes from the middle-south regions of Spain. Biom Bioen. 2007;31:13–9.
11. Park YH, Kim J, Kim SS, Park YK. Pyrolysis characteristics and kinetics of oak trees using thermo- gravimetric analyzer and micro-tubing reactor. Biores Technol. 2009;100:400–5.
12. Kim SS, Kim J, Park YH, Park YK. Pyrolysis kinetics and decomposition characteristics of pine trees. Biores Technol. 2010;101:9797–802.

13. Wongsiriamnuay T, Tippayawong N. Non-isothermal pyrolysis characteristics of giant sensitive plants using thermogravimetric analysis. Biores Technol. 2010;101:5638–44.
14. Sutcu H. Pyrolysis of *Pragmites australis* and characterization of liquid and solid products. J Indust Eng Chem. 2008;14:573–7.
15. Parikh J, Channiwala SA, Ghosal GK. A correlation for calculating elemental composition from proximate analysis of biomass materials. Fuel. 2007;86:1710–9.
16. Jiang G, Nowakowski DJ, Bridgwater AV. A systematic study of the kinetics of lignin pyrolysis. Thermoch Acta. 2010;498:61–6.
17. Iredale PJ, Hatt BW, Overend RP, Milne TA, Mudge LK, Editors, fundamentals of thermochemical biomass conversion. Amsterdam: Elsevier; 1985. p. 143–155.
18. Di Blasi C, Lanzetta M. Intrinsic kinetics of isothermal xylan degradation in inert atmosphere. J Anal Appl Pyrolysis. 1997; 40–41:287–303.
19. Ferdous D, Dalai AK, Bej SK, Thring RW. Pyrolysis of lignins: experimental and kinetics studies. Energy Fuels. 2002;16: 1405–12.
20. Wang J, Wang G, Zhang M, Chen M, Li D, Min F, Chen M, Zhang S, Ren Z, Yan Y. A comparative study of thermolysis characteristics and kinetics of seaweeds and fir wood. Proc Biochem. 2006;41:1883–6.
21. Jiang H, Wang J, Wu S, Wang B, Wang Z. Pyrolysis kinetics of phenol-formaldehyde resin by non-isothermal thermogravimetry. Carbon. 2010;48:352–8.
22. Li D, Chen L, Zhao J, Zhang X, Wang Q, Wang H, Ye N. Evaluation of the pyrolytic and kinetic characteristics of *Enteromorpha prolifera* as a source of renewable bio-fuel from the Yellow Sea of China. Chem Eng Res Desi. 2010;88:647–52.
23. Wongsiriamnuay T, Tippayawong N. Thermogravimetric analysis of giant sensitive plants under air atmosphere. Biores Technol. 2010;101:9314–20.
24. Cuña Suárez A, Tancredi N, César C, Pinheiro P, Irene M. Thermal analysis of the combustion of charcoals from *Eucalyptus dunnii* obtained at different pyrolysis temperatures. J Therm Anal Calorim. 2010;100:1051–4.
25. Gotor FJ, Criado JM, Málek J, Koga N. Kinetic analysis of solid-state reactions: the universality of master plots for analyzing isothermal and nonisothermal experiments. J Phys Chem A. 2000;104:10777–82.
26. Pérez-Maqueda LA, Criado JM, Gotor FJ, Málek J. Advantages of combined kinetic analysis of experimental data obtained under any heating profile. J Phys Chem A. 2002;106:2862–8.
27. Wang XB, Si JP, Tan HZ, Niu YQ, Xu C, Xu TM. Kinetics investigation on the combustion of waste capsicum stalks in Western China using thermogravimetric analysis. J Therm Anal Calorim. 2011. doi:10.1007/s10973-011-1556-z.
28. Zou S, Wu Y, Yang M, Li C, Tong J. Pyrolysis characteristics and kinetics of the marine microalgae *Dunaliella tertiolecta* using thermogravimetric analyzer. Biores Technol. 2010;101:359–65.
29. Orfao JJM, Antunes FJA, Figueiredo JL. Pyrolysis kinetics of lignocellulosic materials-three independent reactions model. Fuel. 1999;78:349–58.
30. Rao TR, Sharma A. Pyrolysis rates of biomass materials. Energy. 1998;23:973–8.
31. López FA, Mercê ALR, Alguacil FJ, López-Delgado A. A kinetic study on the thermal behaviour of chitosan. J Therm Anal Calorim. 2008;91:633–9.
32. Peng WM, Wu QY, Tu PG, Zhao NM. Pyrolytic characteristics of microalgae as renewable energy source determined by thermogravimetric analysis. Biores Technol. 2001;80:1–7.
33. Kumar A, Wang L, Dzenis YA, Jones DD, Hanna MA. Thermogravimetric characterization of corn stover as gasification and pyrolysis feedstock. Biom Bioen. 2008;32:460–7.
34. Li D, Chen L, Yi X, Zhang X, Ye N. Pyrolysis characteristics and kinetics of two brown algae and sodium alginate. Biores Technol. 2010;101:7131–6.
35. Sathitsuksanoh N, Zhu ZG, Templeton N, Rollin J, Harvey S, Zhang YHP. Saccharification of a potential bioenergy crop, *Phragmites australis* (Common Reed), by lignocellulose fractionation followed by enzymatic hydrolysis at decreased cellulase loadings. Indus Eng Chem Res. 2009;48(13):6441–7.
36. Aboulkas A, Harfi KE, Nadifiyine M, Bouadili AE. Thermogravimetric characteristics and kinetic of co-pyrolysis of olive residue with high density polyethylene. J Therm Anal Calorim. 2008;91:737–43.
37. Açıkalın K. Pyrolytic characteristics and kinetics of pistachio shell by thermogravimetric analysis. J Therm Anal Calorim. 2011. doi:10.1007/s10973-011-1714-3.
38. Aboulkas A, Harfi KE, Bouadili AE, Nadifiyine M. Study on the pyrolysis of moroccan oil shale with poly (ethylene terephthalate). J Therm Anal Calorim. 2009;100:323–30.